

This work is on a Creative Commons Attribution 4.0 International (CC BY 4.0) license, <https://creativecommons.org/licenses/by/4.0/>. Access to this work was provided by the University of Maryland, Baltimore County (UMBC) ScholarWorks@UMBC digital repository on the Maryland Shared Open Access (MD-SOAR) platform.

Please provide feedback

Please support the ScholarWorks@UMBC repository by emailing [scholarworks-group@umbc.edu](mailto:scholarworks-group@umbc.edu) and telling us what having access to this work means to you and why it's important to you. Thank you.

# A combined loading transducer for calculating the bending moment and torque in a slender circular beam using the minimum numbers of strain gauges, strain grids, and measurement channels

Bernard J Socha III<sup>1</sup>, Edward T Bednarz III<sup>1</sup> and Wei-Dong Zhu<sup>2</sup> 

## Abstract

The purpose of this work is to develop a new methodology that uses the minimum numbers of strain gauges, strain grids, and measurement channels to calculate the bending moment and torque in a slender circular beam under combined loading from measured strains in it. In general, each independent variable requires a minimum of one independent measurement. Two grids of a single-rosette strain gauge located at  $45^\circ$  and  $-45^\circ$  from the longitudinal axis of the beam are used in conjunction with two measurement channels to gather all measurements and form a combined loading transducer. A theoretical set of equations of the new methodology is developed to minimize numbers of strain grids and measurement channels, and an experimental configuration was tested in a variety of scenarios. Calibration factors were independently developed for the bending moment and torque of the beam by separately loading it in their respective directions. These calibration factors were applied to different combined loading scenarios, where errors were found to be on average 1.6% for moment comparison and 6.7% for torque comparison.

## Keywords

Combined loading, transducer, strain gauge, bending moment, torque

Date received: 10 February 2020; accepted: 30 March 2020

Handling Editor: James Brusey

## Introduction

A transducer is a measuring device that can produce varying electrical outputs when varying loads are applied to a structure.<sup>1</sup> Strain gauges are used to form a transducer in this work. Strain gauges contain small wires arranged in strain grids that experience small changes in resistance when loads are applied to the structure.<sup>2</sup> With external electrical circuitry in each measurement channel of the device and calibration, these resistance changes can be converted to experienced stresses.<sup>3</sup>

A uniaxial strain gauge that contains a single-strain grid, as shown in Figure 1, is the simplest strain gauge

and provides measurement in one direction with a single channel. It can be useful for measuring loading along this direction.<sup>4</sup> Multiple uniaxial strain gauges can be arranged at various positions for more complicated strain measurements. One such advanced case

<sup>1</sup>Wilkes University, Wilkes-Barre, PA, USA

<sup>2</sup>University of Maryland, Baltimore County, Baltimore, MD, USA

### Corresponding author:

Wei-Dong Zhu, University of Maryland, Baltimore County, 1000 Hilltop Circle, Baltimore, MD 21250, USA.

Email: wzhu@umbc.edu



Creative Commons CC BY: This article is distributed under the terms of the Creative Commons Attribution 4.0 License (<https://creativecommons.org/licenses/by/4.0/>) which permits any use, reproduction and distribution of the work

without further permission provided the original work is attributed as specified on the SAGE and Open Access pages (<https://us.sagepub.com/en-us/nam/open-access-at-sage>).

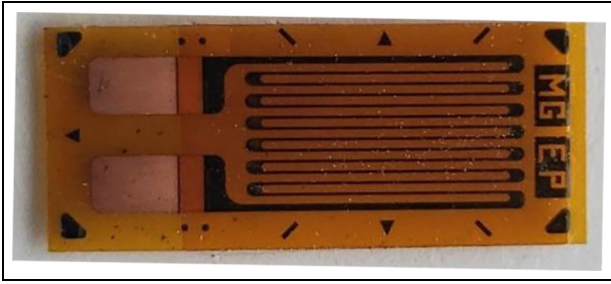


**Figure 1.** Uniaxial strain gauge.

would be using multiple uniaxial strain gauges to build a strain gauge-based force transducer to measure static or dynamic loading on a simply supported beam.<sup>5</sup> It has been shown in Bednarz and Zhu<sup>6</sup> that the strain gauge-based force transducer can be applied to a large-scale bridge. Uniaxial strain gauges can also be utilized to measure static or dynamic pressure.<sup>7</sup> There are two other main types of strain gauge configurations that are shown below.

A shear strain gauge shown in Figure 2 contains two strain grids each of which mounted at  $45^\circ$  off the longitudinal axis of the gauge. It is arranged in a half-bridge configuration, so that only one measurement channel is needed. This configuration allows strain measurements to be subtracted from each other. This is particularly useful in measurement of a torque due to torsional loading, since a torsional stress is directly proportional to the difference of measured strains.<sup>8</sup> If there are enough shear strain gauges on a beam, a strain gauge-based force transducer can be constructed.<sup>9</sup> Locations and magnitudes of multiple applied loads on the beam can then be calculated from measured strains.

A rosette strain gauge shown in Figure 3 contains three strain grids positioned at known angles such as  $45^\circ$ ,  $0^\circ$ , and  $-45^\circ$  off the centerline of the gauge. With three measurements, the maximum and minimum strains can be calculated regardless of the orientation at which the gauge is mounted. However, three separate measurement channels are needed to record strains at these known angles.

Almost all scenarios in real-world applications involve loading along multiple axes. However, loads on cross sections of a slender beam are usually approximated as uniaxial loads on it, due to costs of more transducers needed to measure strains at multiple points of the beam and multiple angles of strain grids. Patent 6,295,878 was issued as a configuration of six strain gauges and six strain grids to measure loading along three axes.<sup>10</sup> Patent 6,354,155 allows for measurement of the force and moment along each of the three axes;<sup>11</sup> however, 12 strain gauges and an equal number of strain grids are needed for this setup. Patent 9,772,237 calculates the magnitude and position of a



**Figure 2.** Shear strain gauge.



**Figure 3.** Rosette strain gauge that contains three strain grids.

load with the use of several strain gauges.<sup>12</sup> A multifunctional sensor network using 27 rosette strain gauges was previously developed.<sup>13</sup>

This work intends to develop and test a new methodology for a combined loading transducer that uses the minimum numbers of strain gauges, strain grids, and measurement channels to calculate the bending moment and torque in a slender circular beam under combined loading from measured strains in it. A single-rosette strain gauge, two strain grids oriented at  $45^\circ$  from the centerline of the gauge that is aligned with that of the beam, and two measurement channels are used. An advantage of the combined loading transducer is that one can calculate two variables, that is, the bending moment and torque in the beam, using strain measurements from only two strain grids and two measurement channels, which are the minimum possible numbers.

The rest of this article is organized as follows: derivation of the theoretical methodology is developed in section "Theoretical methodology" to minimize numbers of strain gauges, strain grids, and measurement channels. An experimental setup is constructed and

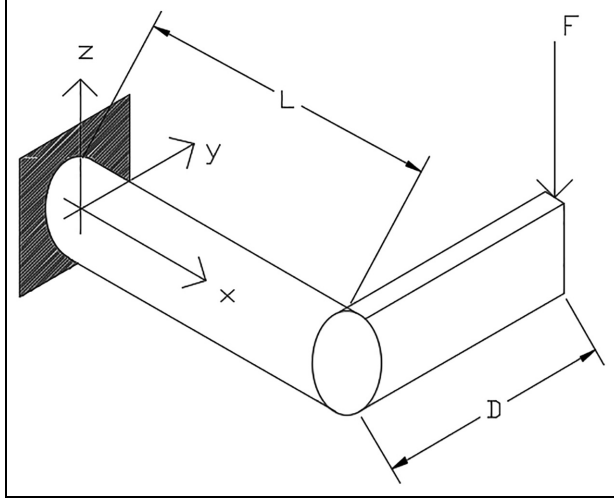


**Figure 4.** Cantilever beam with a loading arm at the end of which a transverse force  $F$  is applied.

calibrated in section “Experimental calibration.” Once calibrated, three different combined loading scenarios are tested: the scenario with an increasing bending moment and torque at the same rate is presented in section “Moment and torque that were increased at equal rates,” that with a constant bending moment and an increasing torque is presented in section “Moment held constant while the torque was increased,” and that with a constant torque and an increasing bending moment is shown in section “Moment was increased while the torque was held constant.” Finally, conclusions are presented in section “Conclusion.”

## Theoretical methodology

Consider a cantilever beam with a loading arm, at the end of which a transverse force  $F$  is applied, as shown in Figure 4. The bending moment  $M$  at the cross section of the beam at the fixed boundary can be written as the product of the transverse force  $F$  and the length of the beam  $L$

$$M = FL \quad (1)$$

The torque  $T$  applied on the beam is

$$T = FD \quad (2)$$

where  $D$  is the length of the loading arm.

When the beam is slender with linear, elastic, and isotropic material, the bending stress  $\sigma_x$  at the top of the cross section of the beam at the fixed boundary is

$$\sigma_x = \frac{Mc}{I} \quad (3)$$

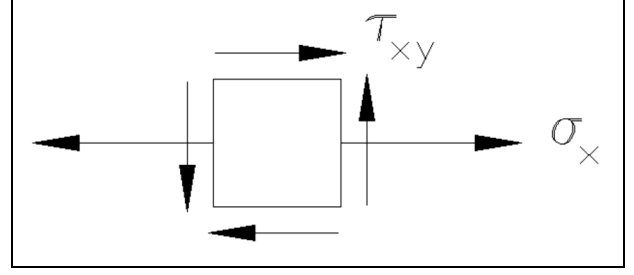


**Figure 5.** Stress element that contains the normal stress  $\sigma_x$  and the shear stress  $\tau_{xy}$ .

where  $c$  is the distance from the neutral axis of the beam to the top of the cross section at which the stress is calculated and  $I$  is the area moment of inertia of the cross section of the beam. A torsional shear stress  $\tau_{xy}$  on a cross section of a beam with a circular cross section can be written as

$$\tau_{xy} = \frac{Tr}{J} \quad (4)$$

where  $J$  is the polar area moment of inertia of the cross section of the beam and  $r$  is the radius of the cross section. While the formula in equation (4) for the torsional shear stress is only applicable for circular cross sections, this methodology can be easily modified for other shapes of cross sections. Equation (4) would be replaced with an applicable relationship between the torque and the shear stress that is valid for the particular shape of a cross section used. For the methodology presented here with a single normal or bending stress  $\sigma_x$  and a shear or torsional stress  $\tau_{xy}$ , the stress element can be seen in Figure 5.

A rosette strain gauge is used in this work to measure strains at the fixed boundary of the beam and calculate the bending moment and torque on it. The strain  $\varepsilon_2$  measured by the middle strain grid in Figure 3 is aligned with the longitudinal or  $x$ -axis of the beam. The strains  $\varepsilon_1$  and  $\varepsilon_3$  measured by the left and right strain grids in Figure 3, located at  $45^\circ$  and  $-45^\circ$  from the longitudinal axis, respectively, can be expressed by

$$\varepsilon_1 = \frac{\sigma'_x}{E} - \frac{\nu\sigma'_y}{E} \quad (5)$$

$$\varepsilon_3 = \frac{\sigma'_y}{E} - \frac{\nu\sigma'_x}{E} \quad (6)$$

where  $E$  is Young's modulus of the beam,  $\sigma'_x$  and  $\sigma'_y$  are normal stresses of the beam at a desired angle of rotation  $\theta$  of strain grids in the  $x$  and  $y$  axes, respectively, as shown in Figure 6, and  $\nu$  is Poisson's ratio.

From the normal bending stress and the torsional shear stress calculated in equations (3) and (4), respectively, a stress tensor  $[\sigma]$  can be created<sup>14</sup>

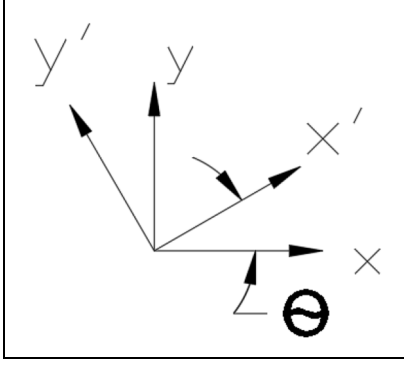


**Figure 6.** Rotation of the  $x$ - $y$  coordinate system in Figure 3 by the angle  $\theta$ .

$$[\sigma] = \begin{bmatrix} \sigma_x & \tau \\ \tau & \sigma_y \end{bmatrix} \quad (7)$$

where  $\sigma_x$  and  $\sigma_y$  are normal stresses of the beam in the  $x$  and  $y$  axes, respectively, and  $\tau$  is the torsional stress of the beam. Since the strain gauges are not aligned to the longitudinal axis, a two-dimensional planar rotation matrix

$$[R] = \begin{bmatrix} \cos(\theta) & \sin(\theta) \\ \sin(\theta) & \cos(\theta) \end{bmatrix} \quad (8)$$

can be used to calculate the rotated normal stress tensor  $[\sigma']$  of the beam at a desired angle of rotation of strain grids

$$[\sigma'] = [R][\sigma][R]^T \quad (9)$$

Due to orientations of the strain grids, desired strains here are for a plane that is rotated  $\theta = 45^\circ$  from the longitudinal axis. Use of equations (7)–(9) yields

$$\begin{bmatrix} \sigma'_x & \tau' \\ \tau' & \sigma'_y \end{bmatrix} = \begin{bmatrix} \cos(45^\circ) & \sin(45^\circ) \\ \sin(45^\circ) & \cos(45^\circ) \end{bmatrix} \begin{bmatrix} \sigma_x & \tau \\ \tau & \sigma_y \end{bmatrix} \quad (10)$$

where  $\tau'$  is the torsional stress of the beam at the desired angle of rotation of the strain grids. Matrix operation in equation (10) yields the following set of equations

$$\sigma'_x = \frac{\sigma_x + \sigma_y}{2} + \tau \quad (11)$$

$$\tau' = \frac{\sigma_y - \sigma_x}{2} \quad (12)$$

$$\sigma'_y = \frac{\sigma_x + \sigma_y}{2} - \tau \quad (13)$$

Since there is no stress applied in the  $y$ -axis, one has

$$\sigma_y = 0 \quad (14)$$

Therefore

$$\sigma'_x = \frac{\sigma_x}{2} + \tau \quad (15)$$

$$\sigma'_y = \frac{\sigma_x}{2} - \tau \quad (16)$$

Substituting equations (15) and (16) into equations (5) and (6), respectively, yields

$$\varepsilon_1 = \frac{(1-\nu)\sigma_x}{2E} + \frac{(1+\nu)\tau}{E} \quad (17)$$

$$\varepsilon_3 = \frac{(1-\nu)\sigma_x}{2E} - \frac{(1+\nu)\tau}{E} \quad (18)$$

Adding equations (17) and (18) yields

$$\varepsilon_1 + \varepsilon_3 = \frac{(1-\nu)\sigma_x}{E} \quad (19)$$

Applying equation (3) to equation (19) yields

$$M = \frac{EI}{c(1-\nu)}(\varepsilon_1 + \varepsilon_3) \quad (20)$$

A linear calibration constant can be used to connect the applied moment and measured strains. The calibration factor for moment is defined by  $\beta_M$ . This calibration factor only depends on geometric and material properties of the beam and should be a constant throughout the experiment that follows. Using a single variable to represent all the known constants allows for easier calculation and demonstration of the methodology

$$\beta_M = \frac{EI}{c(1-\nu)} \quad (21)$$

Applying equations (21) to (20) yields

$$M = \beta_M(\varepsilon_1 + \varepsilon_3) \quad (22)$$

Subtracting equation (18) from equation (17) yields

$$\varepsilon_1 - \varepsilon_3 = \frac{2(1+\nu)\tau}{E} \quad (23)$$

Applying equation (4) to equation (23) yields

$$T = \frac{EJ}{2r(1+\nu)}(\varepsilon_1 - \varepsilon_3) \quad (24)$$

Similarly, a linear calibration constant can be used to connect the torque and measured strains. The calibration factor for the torque is defined by  $\beta_T$ . This calibration factor only depends on geometric and material properties of the beam and should be a constant



**Figure 7.** Experimental setup.

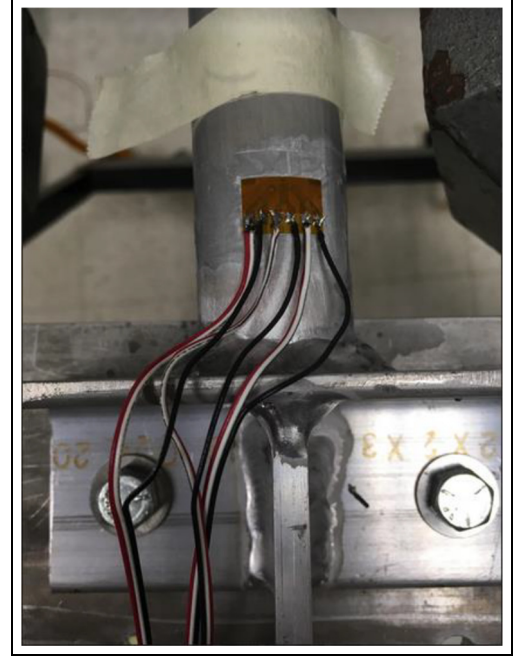


**Figure 8.** Strain gauge located on the cantilever beam.

throughout the experiment that follows. Similar to the procedure for  $\beta_M$ , a single variable is used to represent geometric and material properties of the beam

$$\beta_T = \frac{EJ}{2r(1 + \nu)} \quad (25)$$

Applying equation (25) to equation (24) yields

$$T = \beta_T(\varepsilon_1 - \varepsilon_3) \quad (26)$$

## Experimental investigation

An experiment is conducted on a 31.75 mm outer diameter, 1.59 mm wall thickness, aluminum 6061-T6 round tubing. It is secured on one end to a workbench in a cantilever configuration with a fixed boundary condition, via a fillet weld, and the other end of the round tubing has a loading arm to apply torsional and bending loadings, as shown in Figure 7. The length of each end of the loading arm was 29.53 cm, and the length of the cantilever beam is also 29.53 cm. The rosette strain gauge was positioned at 28.58 mm from the fixed boundary, as can be seen in Figure 8. Consistent with the theory in section “Theoretical methodology,”  $\varepsilon_2$  is aligned with the longitudinal axis of the cantilever beam, as can be seen in Figure 3. Therefore,  $\varepsilon_1$  and  $\varepsilon_3$  are at  $45^\circ$  and  $-45^\circ$  with respect to the longitudinal axis, respectively. The strain gauge wires are connected

to a Vishay P3 strain indicator, which contains an internal Wheatstone bridge circuit.

## Experimental calibration

The first set of experiments was used to calibrate the combined loading transducer. The goal was to find  $\beta_M$  and  $\beta_T$  corresponding to the moment and torque, respectively, which were subsequently used in the rest of the experiments. The maximum error was minimized by adjusting the calibration factors. Microsoft Excel Solver was used in this work, but other applicable software would suffice. The calibration factor  $\beta_M$  was calculated to be equal to 97,731 N m, which is a deviation of  $-12.1\%$  from the theoretical value from equation (21). This is reasonable because of manufacturing tolerances in both the diameter of the shaft and the wall thickness. Young’s modulus and Poisson’s ratio are “known” constants; however, they can vary by small amounts depending on the specific alloy composition.<sup>15</sup>

Moment calibration consisted of two equal weights hanging equidistant from the center of the cantilever beam, as shown in Figure 7. Therefore, positive and negative torques created cancel out and only a moment remains. From experimental data, the applied moment is compared to the sum of measured strains  $\varepsilon_1 + \varepsilon_3$ , as can be seen in Figure 9. A highly linear function can be seen with a slope equal to the optimized  $\beta_M$ .



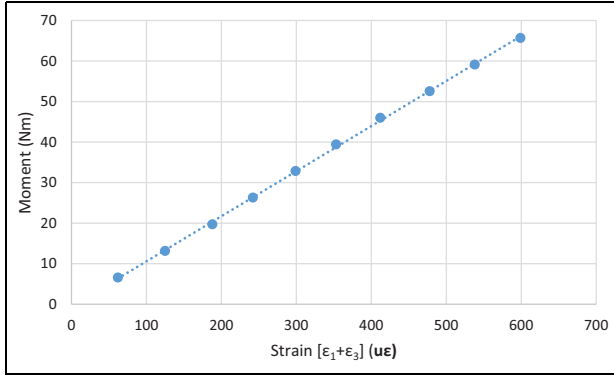


**Figure 9.** Calibration of moment.

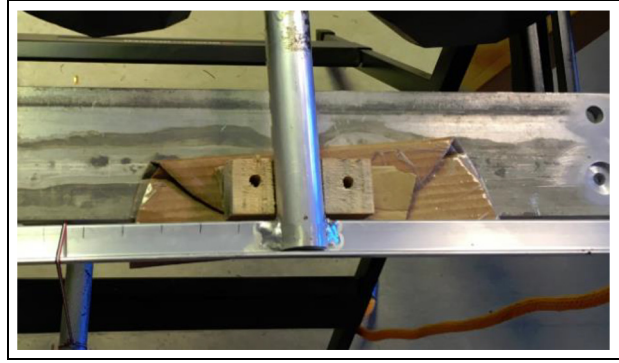


**Figure 11.** Support block.



**Figure 10.** Torque test setup.

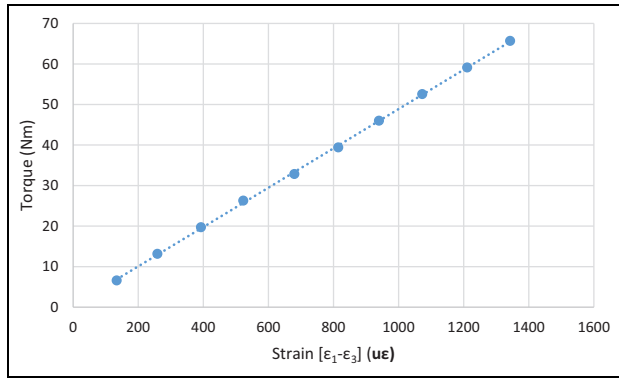


**Figure 12.** Calibration of torque.

Torque calibration was conducted next by hanging a weight on only one side of the loading cantilever beam, as can be seen in Figure 10. A support block was then installed under the center of the cantilever beam to cancel any moment, as shown in Figure 11. Similarly,  $\beta_T$  was found such that there was the lowest maximum error between the calculated torque from the torsional stress and the theoretical torque in equation (2). This was optimized to be 49,500 N m, which is a deviation of  $-11.6\%$  compared to the theoretical value from equation (25). Reasons for this deviation were the same as those described in moment calibration.

From experimental data, the applied torque is compared to the difference of measured strains  $\varepsilon_1 - \varepsilon_3$ , as can be seen in Figure 12. A highly linear function can

be seen with a slope equal to the optimized  $\beta_T$ . Once the calibration factors  $\beta_M$  and  $\beta_T$  were found, other scenarios could be tested using these same values throughout the remaining experiments.

### *Moment and torque that were increased at equal rates*

The first experiment had the torque and moment that were increased at equal rates, which is a combined loading scenario. This was done by hanging a weight to only the left or right side of the loading beam. A weight on the left side of the loading beam can be seen in Figure 13. Measured values of the weight can be seen in Table 1 and calculated values in Table 2.

From calculated combined loading data, the maximum error in the moment measurements was seen to be  $2.9\%$  compared to the theoretical values from equation (1) and the error in the torque was  $5.4\%$  compared to the theoretical values from equation (2). These are both reasonably low for the experimental setup.



**Figure 13.** Combined loading test setup.

#### *Moment held constant while the torque was increased*

The second experiment was also a combined loading scenario; however, this time the moment was held

constant while the torque was increased. This was accomplished by using a single weight of 133 N and varying the distance from the weight to the center on the loading arm, which is similar to what can be seen in Figure 10. Measured values of the weight can be seen in Table 3 and calculated values in Table 4.

The maximum error between the measured moment calculated from equation (22) and the theoretical moment was 3.2%. The maximum error between the measured torque from the torsional stress calculated from equation (26) and the theoretical torque was 14.1%.

#### *Moment was increased while the torque was held constant*

The final experiment was a combined loading scenario where the torque was held constant while the moment was increased. This was accomplished using different weights to create different moments, which is similar to what can be seen in Figure 10. The distance from the weight required to the center of the cantilever beam was then calculated to maintain a constant torque. Measured values of the weight can be seen in Table 5 and calculated values in Table 6.

From calculated combined loading data, the maximum error in the moment measurements was seen to be

**Table 1.** Measured values of the weight from combined loading test with equal moment and torque increments.

Trial number	Mass at left (kg)	Mass at right (kg)	Force (F) (N)	Distance (d) (cm)	Length (L) (cm)	$\varepsilon_1$ ( $\mu\varepsilon$ )	$\varepsilon_3$ ( $\mu\varepsilon$ )
1	2.27	0	22.24	29.53	26.67	100	-39
2	4.54	0	44.48	29.53	26.67	193	-75
3	6.80	0	66.72	29.53	26.67	292	-113
4	9.07	0	88.96	29.53	26.67	402	-158
5	11.34	0	111.20	29.53	26.67	499	-197
6	13.61	0	133.44	29.53	26.67	592	-233
7	15.88	0	155.68	29.53	26.67	697	-273
8	18.14	0	177.92	29.53	26.67	806	-314
9	20.41	0	200.16	29.53	26.67	899	-351
10	22.68	0	222.40	29.53	26.67	1008	-395

**Table 2.** Calculated values of the weight from combined loading test with equal moment and torque increments.

Trial number	Moment (M) actual (N m)	Moment calculated (N m)	Magnitude of moment error	Torque (T) actual (N m)	Torque calculated (N m)	Magnitude of torque error
1	5.93	5.97	0.50%	6.57	6.88	4.60%
2	11.87	11.54	2.90%	13.14	13.27	1.00%
3	17.80	17.49	1.70%	19.71	20.05	1.70%
4	23.73	23.85	0.50%	26.27	27.72	5.20%
5	29.66	29.52	0.50%	32.84	34.45	4.70%
6	35.60	35.10	1.40%	39.41	40.84	3.50%
7	41.53	41.45	0.20%	45.98	48.03	4.30%
8	47.46	48.09	1.30%	52.55	55.45	5.20%
9	53.39	53.57	0.30%	59.11	61.88	4.50%
10	59.33	59.92	1.00%	65.69	69.46	5.40%



**Table 3.** Measured values of the weight from combined loading test with the moment held constant and the varying torque.

Trial number	Mass at left (kg)	Mass at right (kg)	Force (F) (N)	Distance (d) (cm)	Length (L) (cm)	$\varepsilon_1$ ( $\mu\varepsilon$ )	$\varepsilon_3$ ( $\mu\varepsilon$ )
1	13.61	0	133.44	7.62	26.67	300	65
2	13.61	0	133.44	9.53	26.67	333	34
3	13.61	0	133.44	11.43	26.67	355	11
4	13.61	0	133.44	13.34	26.67	385	-18
5	13.61	0	133.44	15.24	26.67	413	-45
6	13.61	0	133.44	17.15	26.67	442	-75
7	13.61	0	133.44	19.05	26.67	465	-98
8	13.61	0	133.44	20.96	26.67	493	-126
9	13.61	0	133.44	22.86	26.67	520	-155
10	13.61	0	133.44	24.77	26.67	549	-184
11	13.61	0	133.44	26.67	26.67	577	-210
12	13.61	0	133.44	28.58	26.67	598	-231

**Table 4.** Calculated values of the weight from combined loading test with the moment held constant and the varying torque.

Trial number	Moment (M) actual (N m)	Moment calculated (N m)	Magnitude of moment error (%)	Torque (T) actual (N m)	Torque calculated (N m)	Magnitude of torque error (%)
1	35.60	35.67	0.20	10.17	11.64	12.60
2	35.60	35.88	0.80	12.71	14.80	14.10
3	35.60	35.78	0.50	15.26	17.03	10.40
4	35.60	35.88	0.80	17.80	19.96	10.80
5	35.60	35.97	1.00	20.34	22.68	10.30
6	35.60	35.88	3.20	22.88	25.59	10.60
7	35.60	35.88	0.80	25.43	27.88	8.80
8	35.60	35.88	0.80	27.97	30.65	8.70
9	35.60	35.67	0.20	30.51	33.41	8.70
10	35.60	35.67	0.20	33.05	36.28	8.90
11	35.60	35.88	0.80	35.60	38.96	8.60
12	35.60	35.88	0.80	38.14	41.04	7.10

**Table 5.** Measured values of the weight from combined loading test with the torque held constant and the varying moment.

Trial number	Mass at left (kg)	Mass at right (kg)	Force (F) (N)	Distance (d) (cm)	Length (L) (cm)	$\varepsilon_1$ ( $\mu\varepsilon$ )	$\varepsilon_3$ ( $\mu\varepsilon$ )
1	13.61	0	133.44	11.43	26.67	356	11
2	11.66	0	114.31	13.34	26.67	339	-9
3	10.21	0	100.08	15.24	26.67	311	-29
4	9.07	0	88.96	17.15	26.67	292	-44
5	8.16	0	80.06	19.05	26.67	284	-58
6	7.44	0	72.95	20.96	26.67	276	-67
7	6.80	0	66.72	22.86	26.67	269	-75
8	6.31	0	61.83	24.77	26.67	255	-80
9	5.85	0	57.38	26.67	26.67	245	-86
10	5.44	0	53.38	28.58	26.67	236	-89

6.2% and the error in the torque was 11.4%. These are both reasonably low for the experimental setup.

## Conclusion

The experiments in this work have proven the methodology of the combined loading transducer. Only one strain gauge, two measurement channels, and two

strain grids were needed to independently measure the moment and torque. Two strain grids of a single-rosette strain gauge were used to accurately calculate the moment from the bending stress and the torque from the torsional shear stress in the combined loading scenarios. Calibration factors were independently found from loading tests of the moment and torque and used throughout other combined loading scenarios.

**Table 6.** Calculated values of the weight for combined loading test with the torque held constant and the varying moment.

Trial number	Moment (M) actual (N m)	Moment calculated (N m)	Magnitude of moment error (%)	Torque (T) actual (N m)	Torque calculated (N m)	Magnitude of torque error (%)
1	35.60	35.88	0.80	15.26	17.07	10.70
2	30.51	32.26	5.40	15.26	17.23	11.40
3	26.69	27.56	3.20	15.24	16.84	9.40
4	23.73	24.24	2.10	15.26	16.63	8.30
5	21.36	22.09	3.30	15.26	16.93	9.90
6	19.42	20.43	4.90	15.26	16.98	10.10
7	17.80	18.96	6.20	15.26	17.03	10.40
8	16.44	17.11	3.90	15.27	16.59	7.90
9	15.27	15.54	1.80	15.27	16.39	6.80
10	14.22	14.37	1.00	15.23	16.09	5.30

The moment had an average magnitude error of 1.6% over the three combined loading scenarios. The torque error was higher at 6.7% mainly due to the system calibration and setup. It is also possible that there was some deflection with the support system at the boundary, allowing for an unaccounted moment in the torque test. While in theory, the cantilever beam is connected to an immovable boundary, in practice there could have been a small deflection at the boundary.


### Declaration of conflicting interests

The author(s) declared no potential conflicts of interest with respect to the research, authorship, and/or publication of this article.

### Funding

The author(s) received no financial support for the research, authorship, and/or publication of this article.

### ORCID iD

Wei-Dong Zhu  <https://orcid.org/0000-0003-2707-2533>

### References

- Bolton W. *Mechatronics electronic control systems in mechanical and electrical engineering*. Harlow: Pearson, 2006.
- Plane-shear measurement with strain gages*. TN-505-4. Malvern, PA: Vishay Measurements Group, Inc, 2010.
- Dorsey J. Homegrown strain-gauge transducers. *Exp Mech* 1977; 17: 255–260.
- Bednarz ET, Zhu WD and Smith SA. Identifying the magnitude and location of a load on a slender beam using a strain gauge based force transducer. *Strain* 2013; 29: 276–285.
- Masroor SA and Zachary LW. Designing an all-purpose force transducer. *Exp Mech* 1991; 31(1): 33–35.
- Bednarz ET and Zhu WD. Identifying magnitudes and locations of loads on slender beams with welded and bolted joints using a strain gage based force transducer with application to a portable army bridge. *J Bridge Eng* 2013; 19(2): 254–264.
- Xu S, Deng X, Tiwari V, et al. An inverse approach for pressure load identification. *Int J Impact Eng* 2010; 37(7): 865–877.
- Plane-shear measurement with strain gages*. TN-512-1. Vishay Measurements Group, Inc., 2010, pp.113–118.
- Bednarz ET, Zhu WD and Smith SA. Identifying magnitudes and locations of multiple loads on a slender beam using strain gage based methods. *J Exp Tech* 2013; 40(1): 15–25.
- Berne N. *Particular strain gauge orientation for a six component load measurement device*. US6295878B1, 2001.
- Berne N. *Multi-component force and moment measuring platform and load transducer*. US6354155B1, 2002.
- Bednarz E and Zhu W. *System for identifying the magnitude and position of a load within a weight area of a beam*. US9772237B1, 2017.
- Chen X, Topac T, Smith W, et al. Characterization of distributed microfabricated strain gauges on stretchable sensor networks for structural applications. *Sensors* 2018; 18(10): 3260.
- Shames IH and Pitarresi JM. *Introduction to solid mechanics*. Upper Saddle River, NJ: Prentice Hall, 2004.
- Bullough CK. *The determination of uncertainties in dynamic Young's modulus. Manual of codes of practice for the determination of uncertainties in mechanical tests on metallic materials*. SMT4-CT97-2165, 2000, pp.1–24, <https://www.npl.co.uk/getmedia/fd2a045b-bc6d-40ac-a38b-3e7a54ac64d4/cop13.pdf>

## Appendix I

### Notation

$c$	distance from the neutral axis of the beam to a location where the strain is measured
$D$	length of the torsional loading arm of the beam from the point where the concentrated force is applied to its vertical axis
$E$	Young's modulus of the beam

$F$	concentrated force applied to the beam	$\varepsilon_3$	strain at $45^\circ$ from the longitudinal axis of the strain gauge
$I$	cross-sectional area moment of inertia of the beam	$\theta$	desired angle of rotation
$J$	cross-sectional polar moment of inertia of the beam	$\nu$	Poisson's ratio of the beam
$L$	distance from the torsional arm of the beam to a location where strains are measured	$[\sigma]$	stress tensor of the beam
$M$	bending moment of the beam at the strain gauge location	$\sigma_x$	normal stress of the beam along the $x$ -axis
$r$	radius of a circular cross section of the beam	$\sigma_y$	normal stress of the beam along the $y$ -axis
$[R]$	rotational matrix of a stress tensor	$[\sigma']$	stress tensor of the beam at a desired angle of rotation of strain grids
$T$	torque of the beam	$\sigma'_x$	normal stress of the beam at a desired angle of rotation of strain grids along the $x$ -axis
$\beta_M$	calibration factor for bending moment calculation	$\sigma'_y$	normal stress of the beam at a desired angle of rotation of strain grids along the $y$ -axis
$\beta_T$	calibration factor for torque calculation	$\tau$	torsional stress of the beam
$\varepsilon_1$	strain at $-45^\circ$ from the longitudinal axis of the strain gauge	$\tau'$	torsional stress of the beam at a desired angle of rotation of strain grids
		$\tau_{xy}$	torsional stress of the beam in the $xy$ plane